AJNR

Optimization of xenon-enhanced CT studies: beam energy, enhancement, root mean square deviation, and repeatability.

K J Kearfott, D A Rottenberg and M D Deck

AJNR Am J Neuroradiol 1983, 4 (2) 195-199
http://www.ajnr.org/content/4/2/195

Optimization of Xenon-Enhanced CT Studies: Beam Energy, Enhancement, Root Mean Square Deviation, and Repeatability

K. J. Kearfott[1]
D. A. Rottenberg[1]
M. D. F. Deck[2]

The effects of varying beam energy on the computed tomographic (CT) enhancement-to-noise (S:N) ratio were studied experimentally with the DeltaScan 2020 and GE 8800 CT scanners and a 20-cm-diameter cyclindrical Plexiglas phantom containing 11 50 ml syringes filled with varying amounts of xenon and iodine. Enhancements of 54.2, 36.7, and 31.7 Hounsfield units (H)/mg I/ml were measured with the DeltaScan 2020 at 70, 100, and 120 kVp, respectively, with corresponding root mean square deviations (RMSDs) of 12, 7, and 5 H for 400 mAs scans. For the GE 8800, enhancements of 48.3, 37.6, and 32.7 H/mg I/ml were measured at 80, 100, and 120 kVp with RMSDs of 13, 8, and 7 H for 9.6 sec 320 mA scans (3.3 msec pulse). RMSD was independent of enhancement over the range of iodine concentrations studied (0–1.5 mg I/ml) and was only a weak function of region-of-interest (ROI) size. For repeated scans with the DeltaScan 2020, measurements in 17 × 17 pixel regions were reproducible to within 0.8 H for all techniques and a drift in calibration of less than 6% was observed after 8 months of clinical use. For both the DeltaScan 2020 and the GE 8800, at the milliamperage studied, lower-energy techniques offered no advantage over 120 kVp technique for xenon CT measurements of regional cerebral blood flow, which are feasible using either of these scanners.

Stable xenon with computed tomography (CT) has been proposed for clinical measurements of regional cerebral blood flow (rCBF) [1–4]. (Xenon is anesthetic when the inspired concentration exceeds 50% [5]; at lower inspired concentrations, sedative effects are minimal or absent [3].) The accuracy and reproducibility of xenon CT rCBF measurements are critically dependent on the xenon enhancement-to-noise (or signal-to-noise, S:N) ratio [6]. Further, xenon enhancement and image noise are both functions of the CT beam energy used. ("Enhancement" refers to an increase in CT number due to the presence of stable xenon or other contrast medium.) To optimize CT scanning technique for clinical xenon CT rCBF studies and to estimate errors due to machine calibration and image noise, the effects of varying kilovoltage on enhancement and root mean standard deviation (RMSD) must be determined over the range of enhancements with clinically feasible CT techniques. The enhancement/RMSD ratio was found to be maximal at 90–100 kVp for both the EMI Mark I [7] and the EMI 1010 [8], for which it was possible to increase the milliamperage for the lower-energy scans to maintain constant heat load.

Our interest in xenon CT [4, 6] led us to: (1) measure the enhancement/RMSD ratio for the DeltaScan 2020 and GE 8800 CT scanners, (2) determine the standard deviation of repeated CT measurements, and (3) examine the effects of region-of-interest (ROI) size and reconstruction matrix on RMSD.

Received June 15, 1982; accepted after revision October 20, 1982.

This work was supported in part by HEW Public Health Service grant NS 15665.

[1]Department of Neurology, Memorial Sloan-Kettering Cancer Center, 1275 York Ave., New York, NY 10021. Address reprint to K. J. Kearfott.

[2]Department of Radiology, Memorial Sloan-Kettering Cancer Center, New York, NY 10021.

AJNR 4:195–199, March/April 1983
0195–6108/83/0402–0195 $00.00

Theory

CT Enhancement

The observed enhancement or increase in CT number, E, in Hounsfield units (H) due to the presence of a contrast medium i may be determined from:

$$E = \frac{1{,}000(\mu/\rho)_i C_i}{\mu_w}, \quad (1)$$

where μ_w is the linear attenuation coefficient of water and $(\mu/\rho)_i$ and C_i are the mass attenuation coefficient and concentration of i, respectively. As the effective energy of the CT x-ray spectrum approaches the K-absorption edge (34.6 keV for xenon), μ/ρ peaks, and E is therefore maximized. Hence, enhancement should increase as CT beam energy decreases from 120 kVp to 70 kVp and lower.

CT Noise and Repeatability

The observed "noise" in a CT image reflects radiation quantum variations, tissue inhomogeneity, and the effects of CT reconstruction and image processing. In conventional CT scans, quantum noise dominates over the contribution of tissue inhomogeneity [9]. Further, the observed noise is extremely dependent on scanning technique (including the milliamperage and beam energy) and reconstruction filtering [10].

For the same milliamperage, CT noise will increase if the effective beam energy is decreased because of greater beam attenuation and consequent worsening of quantum statistics. Since tube heating limitations, short scanning times required for xenon CT rCBF studies, and the available repertoire of machine calibrations effectively constrain CT technique, only selected Delta-Scan 2020 and GE 8800 techniques will be considered.

The variance for a ROI of N pixels will be taken as a measure of CT noise:

$$(RMSD)^2 = \frac{\Sigma_i^N(\bar{H} - H_i)^2}{(N-1)}, \quad (2)$$

where RMSD is the pixel root mean square deviation, $\bar{H}$ is the mean Hounsfield number for the region, and H_i is the Hounsfield number for the i^{th} pixel.

As defined above, the variance is nearly constant over the range of CT numbers of interest [11]. The proportional error (PE) in measured xenon enhancement, E, for a ROI containing N pixels may be estimated as [12]:

$$PE = \frac{2^{1/2} \cdot RMSD}{E \cdot N^{1/2}}, \quad (3)$$

where the $2^{1/2}$ factor reflects the subtraction of two independent measurements (enhanced scan − baseline scan) with the same RMSD. The repeatability of a measurement may be determined by taking the standard deviation of the mean of a number of different scans.

Figure-of-Merit for Xenon CT rCBF Studies at Different Energies

The suitability of a given CT technique depends not only on the observed change in enhancement for a given change in xenon concentration but also on the noise inherent in such measurements. The slope of the CT enhancement/RMSD curve as a function of contrast concentration should therefore serve as a figure-of-merit for comparing the use of different energies for xenon CT rCBF studies. This figure-of-merit (FOM), which is relatively independent of observed enhancement (thus facilitating the comparison of data from different sources), is given by:

$$FOM = \frac{E}{(RMSD \cdot C)}, \quad (4)$$

where C represents the concentration of xenon in mg/ml.

Methods

A 20-cm-diameter cylindrical Plexiglas phantom was constructed with 11 radially disposed holes for 50 ml syringes. Either iodine, in the form of metrizamide (0.05–1.5 mg I/ml), or xenon gas (0.1–0.6 mg Xe/ml) was added to normal saline to cover the range of contrast enhancement expected in clinical xenon CT rCBF studies. Two nonenhanced saline references were included. CT scans with the DeltaScan 2020 were taken at 70, 100, and 120 kVp for both 256 × 256 (400 mAs) and 512 × 512 reconstruction matrices (400 and 800 mAs). For the GE 8800, scans at 80, 100, and 120 kVp were obtained (9.6 sec, 320 mA, 3.3 msec pulsed source, 320 × 320 reconstruction matrix). ROIs (17 × 17 to 21 × 21 pixels, with each pixel 1 × 1 mm) were placed within the areas corresponding to the syringes.

Ten rapid (every 1–2 min) sequential scans of the phantom with metrizamide and five sequential scans of a 20-cm-diameter uniform water phantom were also obtained at 70, 100, and 120 kVp using the DeltaScan 2020. Thirty-six ROIs varying in size from 8 × 8 to 174 × 174 pixels were centered on the water phantom in order to determine the dependence of RMSD on ROI size. Pixel regions of 18 × 18 were centered in the water phantom scans to examine measurement reproducibility.

Theoretical estimates of enhancement for the DeltaScan 2020 based on effective energies of 51, 62, and 70 keV with 70, 100, and 120 kVp beams [13] were made. Mass attenuation coefficients were computed by interpolating the available data [14] for both energy and atomic number. A solubility of 0.107 cc/g for xenon in 0.9% NaCl at 25°C [15] and a density of 5.15 mg/ml, corrected for ambient temperature and pressure, were used to compute the xenon concentration.

Results

Iodine and Xenon Enhancements

At all three energies the average measured enhancement for iodine differed from the predicted enhancement by less than 6 H. These results agree well with observed differences of less than 10 H for elements of atomic number below 60 [13]. Predicted and measured enhancement differed by less than 8 H for xenon. The observed average enhancement/ml/mg iodine and xenon differed by 7.1% at 120 kVp,

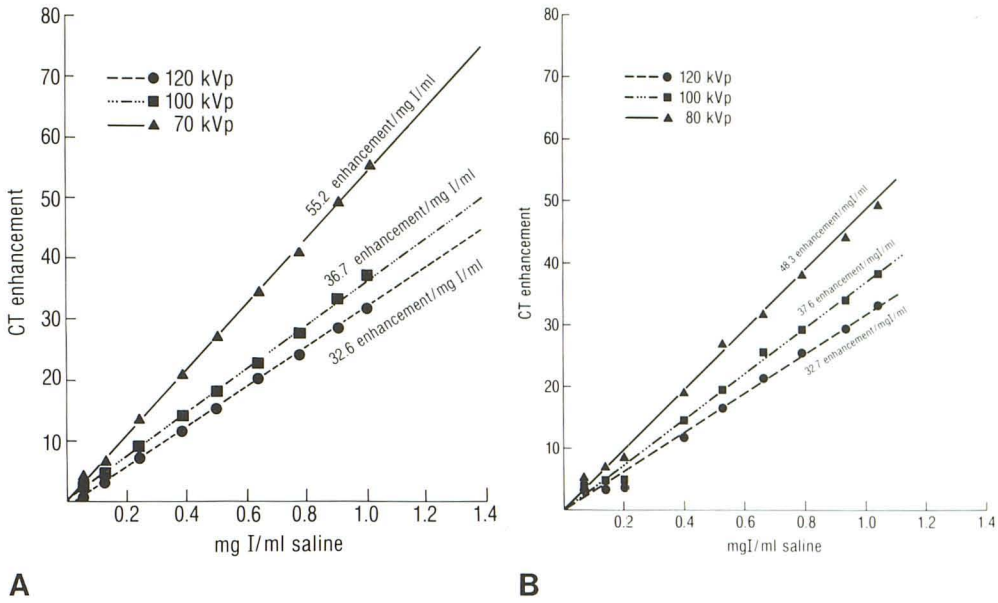

Fig. 1.—CT enhancement as a function of iodine concentration for the DeltaScan 2020 at 70, 100, and 120 kVp spectra (**A**) and for the GE 8800 at 80, 100, and 120 kVp spectra (**B**).

compared with the theoretical prediction of 2.4%. The larger observed difference is attributed to variations in the concentration of test solutions and inaccuracies in the xenon solubility data.

The CT enhancement data is plotted as a function of iodine concentration in figure 1A for the DeltaScan 2020 and in figure 1B for the GE 8800. The corresponding best fits to the experimental data ($r^2 > 0.97$ for all curves) are included. The calibrations at 70, 100, and 120 kVp were measured as 55.2, 36.7, and 32.6 H enhancement/mg I/ml for the DeltaScan 2020 and 48.3, 37.6, and 32.7 H enhancement/mg I/ml for the GE 8800 at 80, 100, and 120 kVp. After 8 months, during which time the DeltaScan 2020 was in continuous clinical use and underwent a change of x-ray tubes with associated retuning, a repeat experiment reproduced earlier calibration values to within 5.8% at all three energies. Adding a parabolic aluminum filter (thickness varying from 4 mm to several centimeters at the edge) to the DeltaScan 2020 changed the calibration by 5%–7% for the range of iodine concentrations studied.

RMSD

No correlation was observed between CT enhancement and RMSD for the small enhanced regions in the Plexiglas phantom. Average RMSDs for the DeltaScan 2020 with 400 mAs scans was 10–13 H at 70 kVp, 6.2–7.4 H at 100 kVp, and 4.8–5.1 H at 120 kVp for the metrizamide-filled phantom with 18 × 18 pixel ROIs. For the water phantom, RMSDs of 14.8, 7.9, and 6.3 for equivalent ROIs at 70, 100, and 120 kVp were observed (these are about 9%–12% higher than those observed in the metrizamide phantom). The corresponding variations due to placement of the ROIs in the center of the uniform water phantom were 0.5, 0.2, and 0.1 H.

As expected, the measured RMSD for the uniform water phantom was only a weak function of ROI size for ROIs greater than 7 × 7 pixels. For the 120 kVp scan at 400 mAs with the DeltaScan 2020 the data was fit by

$$RMSD = 7.016 - 0.00931\ N^{1/2} (r^2 = 0.966), \quad (5)$$

where N is the number of ROI pixels. Similar results were observed at the other energies. Repeated measurements with the DeltaScan 2020 separated by an 8 month period revealed variations in the measured RMSD of 1%–24%, but the larger variations in RMSD are believed to be due to ROI and phantom positioning and regional variations in RMSD rather than to machine performance changes.

Scans with the DeltaScan 2020 at 200 mAs had RMSDs 2.3 times those at 400 mAs, while 800 mAs scans produced only a 15% improvement in RMSD for 512 × 512 reconstructions. For 70 and 100 kVp, increasing the milliamperage from 400 to 800 mAs decreased the RMSD by a factor of about 2. ROIs in the metrizamide phantom scanned with the GE 8800 had RMSDs of 12–14, 7.8–9.0, and 6.2–6.8 H at 80, 100, and 120 kVp.

Relative Merit of 70 or 80, 100, and 120 kVp Techniques

Table 1 summarizes the figures of merit for the DeltaScan 2020 and GE 8800 techniques studied. For the DeltaScan 2020, reconstructing at 256 × 256 did not substantially improve the S:N for scans done at 120 kVp but did improve this ratio significantly for 70 and 100 kVp scans. At 400 mAs with 512 × 512 reconstruction, the 120 kVp technique

TABLE 1: **Enhancement-to-Noise (S:N) Ratios of 70–80, 100, and 120 kVp Techniques**

CT Technique (kVp)	DeltaScan 2020					GE 8800
	200 mAs	400 mAs			800 mAs	9.6 sec 320 mA
	512*	512*†	512*†	256*	512*	320*
120	4.7	10.8	9.9	11.0	12.4	5.0
100	...	6.0	6.6	10.5	13.5	4.5
80	...	...	...	...	...	3.6
70	...	5.1	4.6	8.9	10.4	...

Note. S:N ratio = (CT enhancement/RMSD)/(mg I/ml saline).
* Reconstruction matrix.
† Repeated measurements separated by 8 months.

TABLE 2: **Proportional Error in Enhancement Measurements**

Scanner	Pixels	70 kVp	100 kVp	120 kVp
DeltaScan 2020 (400 mAs, 512 × 512):				
0.05 mg Xe/ml	100	0.615	0.471	0.262
	200	0.435	0.333	0.185
0.10 mg Xe/ml	100	0.307	0.236	0.131
	200	0.217	0.167	0.093
0.15 mg Xe/ml	100	0.205	0.157	0.087
	200	0.145	0.111	0.062
Scanner	**Pixels**	**80 kVp**	**100 kVp**	**120 kVp**
GE 8800 (320 mA, 9.6 sec, 3.3 msec pulse):				
0.05 mg Xe/ml	100	0.786	0.629	0.566
	200	0.556	0.444	0.400
0.10 mg Xe/ml	100	0.393	0.314	0.283
	200	0.278	0.222	0.200
0.15 mg Xe/ml	100	0.262	0.210	0.189
	200	0.185	0.148	0.133

was clearly superior to the other DeltaScan 2020 techniques studied.

For a 256 × 256 reconstruction with the DeltaScan 2020, there was little difference between 100 and 120 kVp techniques. At 800 mAs there was an overall improvement of about 10% in the S:N ratio; however, the longer scanning time needed to achieve these statistics is suboptimal for xenon CT rCBF measurements, both in terms of temporal sampling and the possible introduction of temporal artifacts [16]. The increase in noise at 70 kVp precludes any advantages arising from an increase in enhancement at this beam energy for the techniques studied.

For the GE 8800 techniques studied, the 120 kVp technique seemed superior at the given milliamperage. Figures-of-merit were generally lower for the GE 8800 than for the DeltaScan 2020, but it should be remembered that this is a function of effective milliamperage as well as reconstruction parameters.

Repeatability and Precision of Measurements

Like the RMSD, the repeatability (standard deviation of several measurements) was found not to be a function of the iodine concentration or enhancement in the small subregions of the phantom. For the 17 × 17 pixel regions in the metrizamide phantom, the various enhancements were reproduced to within 0.78, 0.27, and 0.34 H for 10 repeated scans at 70, 100, and 120 kVp, respectively; for five scans of the water phantom, repeatabilities of 0.26, 0.16, and 0.13 H were achieved at these energies. No systematic drifts were observed.

Estimate of Proportional Error in Enhancement Measurements

Table 2 summarizes the proportional error, estimated using equation 3, for different concentrations of xenon and ROI size for xenon CT enhancement based on the measured RMSD and CT calibration for both the DeltaScan 2020 and the GE 8800. The superiority of the 120 kVp technique is apparent.

Discussion

With both the DeltaScan 2020 and GE 8800 CT scanners, measured iodine or xenon enhancement correlated well with that predicted based on the equivalent energy of the CT beam. The calibration of the DeltaScan 2020 for xenon CT rCBF studies was amazingly stable (within 6%) over an 8 month period.

The RMSD of pixel values was independent of the magnitude of enhancement and ROI size over the range of iodine and xenon concentrations studied. For the CT techniques studied, any advantage in enhancement at lower energies was overwhelmed by noise. With constant heat load, however, lower energy techniques are superior [7, 8]. The observed RMSD may be reduced by increasing milliamperage, reconstructing with a coarser matrix, or by employing special reconstructing filtering or front-end smoothing. Regional variations in RMSD may be minimized (although not completely eliminated) by careful machine calibration.

Excellent repeatability and an absence of systematic drift were observed for the DeltaScan 2020 during rapidly repeated scan sequences similar to those used for xenon CT rCBF measurements. Standard deviations for series of rapid-fire scans were less than 0.8 H for all three techniques studied. The impressive stability and favorable signal-to-noise characteristics of the of the DeltaScan 2020 and GE 8800 CT scanners allow for accurate CT measurements of rCBF during stable xenon inhalation.

ACKNOWLEDGMENTS

We thank Vijay Dhawan (Department of Neurology, Memorial Sloan-Kettering Cancer Center) and Victor Haughton (Department of Radiology, Medical College of Wisconsin, Milwaukee) for providing scans with the GE 8800; and Paula Carmichael (New York University, New York) for assistance with data analysis.

REFERENCES

1. Winkler SS, Sacket JF, Holden JE, et al. Xenon inhalation as an adjunct to computerized tomography of the brain: preliminary study. *Invest Radiol* **1977**;12:15–18
2. Drayer BF, Dujorny M, Wolfson SK, et al. Xenon- and iodine-enhanced CT of diffuse cerebral circulatory arrest. *AJNR* **1980**;1:227–232
3. Meyer JS, Hayman LA, Yamamoto M, Sakai F, Nakajima S.

Local cerebral blood flow measured by CT after stable xenon inhalation. *AJNR* **1980**;1:213–225

4. Rottenberg DA, Goldiner P, Dhawan V, Kearfott KJ. Measurement of regional cerebral blood flow in human subjects using stable xenon and computerized tomography. *Trans Am Neurol Assoc* (in press)
5. Cullen SC, Gross EG. The anesthetic properties of xenon in animals and human beings, with additional observations on krypton. *Science* **1951**;113:580–582
6. Rottenberg DA, Lu HC, Thaler HT, Kearfott KJ. The measurement of rCBF using CT and stable xenon. *J Cerebral Blood Flow Metab* **1981**;1(Suppl 1):527–528
7. Kelcz F, Hilal SK, Hartwell P, Joseph PM. Computed tomographic measurement of the xenon brain-blood coefficient and implications for regional cerebral blood flow: a preliminary report. *Radiology* **1978**;127:385–392
8. Keller MR, Kessler RM, Brooks RA, Kirkland LR. Optimum energy for performing CT iodinated contrast studies. *Br J Radiol* **1980**;53:576–579
9. Duerinckx AJ, Macovski A. Information and artifact in computed tomography image statistics. *Med Phys* **1980**;7:127–134
10. Hemmingsson A, Jung B, Ytterbergh C. Noise and noise texture in CT images before and after post-processing. *Acta Radiol [Diagn]* **1980**;21:807–812
11. Thaler HT, Lu, HC, Rottenberg DA. Technique for locating homogeneous regions within CT brain slices. *AJNR* **1980**;1:475–476
12. Rottenberg DA, Lu HC, Kearfott KJ. The *in vivo* autoradiographic measurement of regional cerebral blood flow using stable xenon and computerized tomography: the effect of tissue heterogeneity and computerized tomography noise. *J Cerebral Blood Flow Metab* **1982**;2:173–178
13. Judy PF, Adler GJ. Comparison of equivalent photon energy calibration methods in computed tomography. *Med Phys* **1980**;7:685–691
14. Evans R. "X-ray and γ-ray interactions". In: FH Attix, Roesch WC, eds. *Radiation dosimetry*, vol 1: *Fundamentals*, 2d ed, New York: Academic Press, **1968**:93–155
15. Yeh SY, Peterson RE. Solubility of carbon dioxide, krypton and xenon in aqueous solutions. *J Pharm Sci* **1964**;53:822–824
16. Wingfat RI. *Local cerebral homodynamics by tracing stable xenon with transmission computed tomography* (Ph.D. dissertation). Madison, WI: University of Wisconsin, **1981**